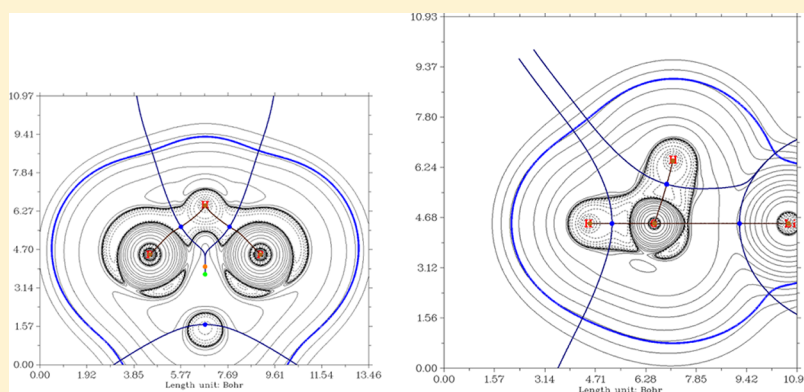


Do Organometallic $\text{CH}_4\text{--Me}^{+p}$ Adducts and X_4H^+ ($\text{X} = \text{P}, \text{As}$) Clusters Undergo Two-Electron Three-Center Interactions? Some Aspects of Discussion

Rosana M. Lobayan^{†,*} and Roberto C. Boichichio^{‡,*}

[†]Departamento de Física, Facultad de Ciencias Exactas, Naturales y Agrimensura, Universidad Nacional del Nordeste, 3400, Corrientes, Argentina

[‡]IFIBA-CONICET and Departamento de Física, Facultad de Ciencias Exactas y Naturales, Universidad de Buenos Aires, Ciudad Universitaria, 1428, Buenos Aires, Argentina



ABSTRACT: Most of the systems possessing true two-electron three-center interactions are electron deficient compounds like boron hydrides, *closo*-boranes, and some organic ions such as butonium cations. In this work, we perform a detailed study of the electron distribution for two different types of systems to which likewise interactions has been adjudicated: organometallic $\text{CH}_4\text{--Me}^{+p}$ ($p = 1, 2$) adducts with Me, alkaline and earth alkaline metallic ions of Li, Na, K, Be, Mg, Ca in their stable gaseous phase and X_4H^+ ($\text{X} = \text{P}, \text{As}$) simple clusters. For this purpose, topological analysis of the electron density decomposed into its effectively paired and unpaired contributions has been carried out looking for complex interactions.

1. INTRODUCTION

The understanding of the chemical interactions has become a field of active research because of the advent of the new theories about the behavior of the entities like atoms in the molecular context and the capacity of the computational tools to calculate the details of these phenomena.^{1,2} The complete information about a molecular system is immersed in the electron density³ which may be straightforwardly obtained from Kohn–Sham density functional theory (DFT)⁴ or from the very state function by contraction of the reduced density matrices.⁵ The most rigorous formalism to search the above-mentioned information is based in the Lagrangian quantum mechanics which enables to define an atom in a molecular framework.^{1,2} The aims of the techniques derived from this formalism is to go beyond the description of the classical structures in order to penetrate each of the classes in which the unobserved concept of chemical bond demises space to the general concept of chemical interactions. This is directly related to the difficulties to characterize and unify the wide variety of which is called chemical bond.⁶ In this respect, we have introduced a methodology to appropriately describe the different types of chemical interactions what we called a

quantum version of the Lewis model.^{7,8} This technique enabled us to go beyond the traditional chemical structures. Applications has been performed for the classical structures of chemical compounds as well as to more complex systems looking for the detection and detailed description of complex patterns of bonding ranging from electron deficient compounds like boron hydrides^{9–11} to molecular organic ions.¹² All them are recognized to possess two-electron three-center (2e–3c) interaction mechanisms. This method supplied us of a strong support for the description and the later understanding of this phenomenon.

Within this scenario in the present report we apply our methodology to two different type of systems which has been pointed out in the literature as candidates to undertake 2e–3c interactions, in our opinion with not enough theoretical arguments: adducts $\text{CH}_4\text{--Me}^{+p}$ ($p = 1, 2$) with Me, metallic ions of alkaline and earth alkaline metals Li, Na, K, Be, Mg, Ca in their stable gaseous phase^{13,14} and simple metalloid clusters

Received: April 4, 2015

Revised: June 9, 2015

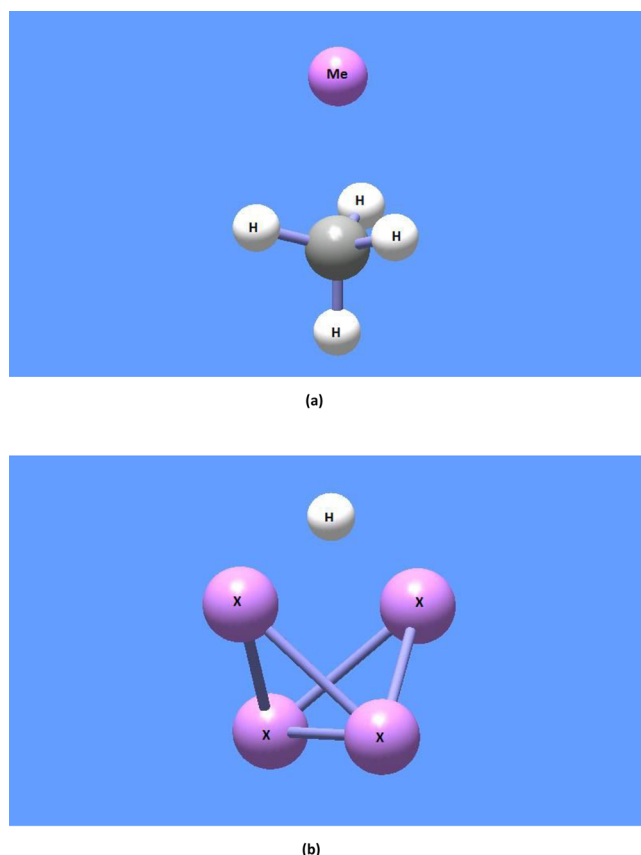


Figure 1. Geometrical conformation: (a) CH_4Me^+ adducts; (b) X_4H^+ clusters.

X_4H^+ ($\text{X} = \text{P}, \text{As}$).^{15–17} The importance of the first group, i.e., organometallic adducts, resides in the kind of interaction between the C atoms and the metallic ion, recognized by the chemical inertness of CH bonds in alkanes which however has been reported as reactive under certain circumstances.^{13,14} There should be not enough electrons available for a covalent interaction between carbon atom and the metallic ion for a subsequent bond formation and in this sense these systems may be considered as electron deficient. The second group provides an interesting example for metalloid patterns for chemical interactions^{15,16} which as well as first group conforms a set of electron deficient systems. For this reason, these systems offer an encouraging possibility to probe the question for 2e–3c chemical interactions. The treatment of these systems provide a high experience for both the application of the density decomposition model and the essential role of correlation effects on the electron distribution.

The aim of this report is to describe the electronic distribution of the mentioned selected molecular systems in detail by application of the topological analysis of the electron density from the point of view of its decomposition into paired ($\rho^{(p)}(\mathbf{r})$) and unpaired ($\rho^{(u)}(\mathbf{r})$) contributions each of them with a different and definite physical character^{7,8} to interpret and further classify the distributions by means of interaction types.¹² To this end, the information contained in the N -electron state function is transferred toward the fundamental chemical concepts^{18–22} in the qualitative and quantitative manner by means of the electron density.^{23,24} Two complementary views within the topological framework are used to assess the information in the density and its

contributions. On one side, the *local formulation* relates the topological structure of the electron density $\rho(\mathbf{r})$ and its Laplacian field $\nabla^2\rho(\mathbf{r})$ to the localization and classification of their critical points (**cp**) which characterize these fields and therefore permits to extract and interpret the chemical information as chemical interactions.^{1,2} On the other side, the *nonlocal or integrated formulation* counterpart currently known as electronic population analysis²⁵ has several implementations which permit to determine and interpret the chemical fundamental quantities like covalent bond orders, valence and atomic populations among others²⁰ which acts as the complement of the local formulation. The detailed analysis and comparison of the information coming from the density fields over several different type of compounds^{7,8,10–12} allowed to define two types of interactions regarding the spatial domain of accumulation of the unpaired density. If it is close to the bond paths between atoms the interaction will be called *through bond* (TB); if there are “spillages” through the space beyond the bond path of interacting atoms, making it consequently strongly delocalized in space, the interaction will be called *through space* (TS).¹²

The organization of this article is as follows. The second section is devoted to a brief introduction to the theoretical methodology of the topological analysis of the electron density, the relationships between the density gradients and the Laplacians, as well as the tools used to carry out the studies of topological population analysis. The third section describes the computational details and the discussion of the results. The final section is dedicated to the concluding remarks.

2. THEORETICAL ASPECTS

The electron density $\rho(\mathbf{r})$ of a N -electron molecular system may be decomposed into two contributions,^{7,8} i.e., $\rho(\mathbf{r}) = \rho^{(p)}(\mathbf{r}) + \rho^{(u)}(\mathbf{r})$ where $\rho^{(p)}(\mathbf{r})$ and $\rho^{(u)}(\mathbf{r})$ indicate the effectively paired and unpaired densities, expressed by

$$\rho^{(p)}(\mathbf{r}) = \frac{1}{2} \int d\mathbf{r}' {}^1D(\mathbf{r}|\mathbf{r}') {}^1D(\mathbf{r}'|\mathbf{r}), \quad \rho^{(u)}(\mathbf{r}) = \frac{1}{2} u(\mathbf{r}|\mathbf{r}) \quad (1)$$

respectively. ${}^1D(\mathbf{r}|\mathbf{r}')$ stands for the spin-free first-order reduced density matrix (1-RDM) in spatial coordinate representation,^{23,24} its trace (coordinate integration over the whole space) is the number of electrons in the system, i.e., $\text{Tr}({}^1D) = \int d\mathbf{r} {}^1D(\mathbf{r}|\mathbf{r}) = \int d\mathbf{r} \rho(\mathbf{r}) = N$. $u(\mathbf{r}|\mathbf{r})$ is the diagonal element of the effectively unpaired density matrix $u(\mathbf{r}|\mathbf{r}') = 2 {}^1D(\mathbf{r}|\mathbf{r}') - {}^1D^2(\mathbf{r}|\mathbf{r}')$ where ${}^1D^2(\mathbf{r}|\mathbf{r}') = \int d\mathbf{r}'' {}^1D(\mathbf{r}|\mathbf{r}'') {}^1D(\mathbf{r}''|\mathbf{r}')$.^{7,8,24} The densities are the diagonal part of the corresponding reduced density matrices.^{23,24} The physical meaning of the effectively paired and unpaired densities are related to the difference of the orbital occupation from the double occupancy due to the spin state and the electron correlation. The unpaired density $\rho^{(u)}(\mathbf{r})$ has two sources, one of them comes from the spin density (only present in nonsinglet states) and the other corresponds to the correlation effects,²⁶ and then it is intrinsically zero^{27–30} for single determinant state functions having all doubly occupied orbitals. Consequently the local finer details from correlation effects can not be properly detected from these type of descriptions.

The fundamental information for the topological analysis is related to the nature and localization of the cp's of the two electron densities and their local accumulation/depletion around them in space.^{1,2} The cp's for the total density are determined throughout the gradient of the field by

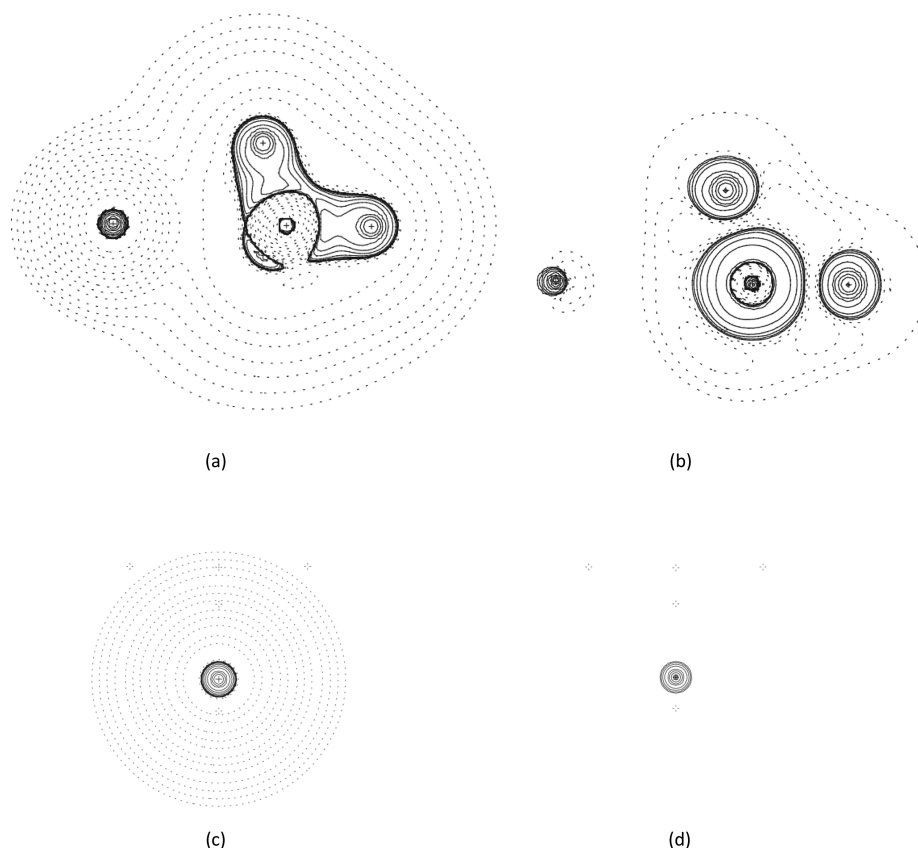


Figure 2. $L(\mathbf{r})$ contour maps for total density (a) and effectively unpaired densities (b) in the plane defined by C, Li ion and two of the closest H atoms and (c and d) total and effectively unpaired densities of the isolated metal ion, respectively. Positive and negative values are denoted by solid and dashed lines, respectively.

$$\nabla \rho(\mathbf{r})|_{\mathbf{r}^c} = 0, \quad \nabla \rho^{(p)}(\mathbf{r})|_{\mathbf{r}^c} + \nabla \rho^{(u)}(\mathbf{r})|_{\mathbf{r}^c} = 0 \quad (2)$$

where $\mathbf{r}^c = \{\mathbf{r}_i^c; i = 1, \dots, M\}$ stands for the set of critical points of $\rho(\mathbf{r})$. Thus, $\nabla \rho^{(p)}(\mathbf{r})|_{\mathbf{r}^c} = -\nabla \rho^{(u)}(\mathbf{r})|_{\mathbf{r}^c}$ indicates that both parts increase its value in the opposite direction. The cp's are featured as (r, s) , where r is the *rank* (nonzero number of eigenvalues of the Hessian matrix of $\rho(\mathbf{r})$) and s the *signature* (sum of the signs of its eigenvalues). The points of interest are the nuclear critical point (**ncp**) $(3, -3)$, which indicates a local maximum placed very close to the nuclear positions; the $(3, -1)$, bond critical point (**bcp**) where its existence and concentration of the electron density shows a bonding interaction between two atoms.^{1,2} The remaining cp's, *ring*, (**rcp**) and *cage*, (**ccp**) critical points, indicate the onset of more complex structures and are noted as $(3, +1)$ and $(3, +3)$, respectively.^{1,2} The behavior of the density around a point in space is described by the modulus and sign of the Laplacian field which indicates locally depletion (positive) or locally concentration (negative) of the electron density.^{1,2} The Laplacian field decomposition $\nabla^2 \rho(\mathbf{r})|_{\mathbf{r}^c} = \nabla^2 \rho^{(p)}(\mathbf{r})|_{\mathbf{r}^c} + \nabla^2 \rho^{(u)}(\mathbf{r})|_{\mathbf{r}^c} \neq 0$ may be interpreted as that both contributions, $\nabla^2 \rho^{(p)}(\mathbf{r})|_{\mathbf{r}^c}$ and $\nabla^2 \rho^{(u)}(\mathbf{r})|_{\mathbf{r}^c}$ do not necessarily follow opposite trends, as the density gradient does; i.e., both densities are allowed to concentrate or deplete simultaneously at the neighborhood of a **cp**. Complementary to the *local formalism*, the *nonlocal* or *integrated formalism* incorporates the quantum expressions for the classical chemical concepts like atomic charges, covalent bond orders and valences, etc.^{18–22} We will refer to information contained in these quantities as the AIM (atoms in molecules) topological population analysis based in

Bader's theory.^{18–22} The more relevant magnitudes within that approach which will be used in our study^{20–22,31–33} are the covalent bond order (two-center bond index)

$$I_{\Omega_A \Omega_B} = \sum_{i,j,k,l} {}^1D_j^i {}^1D_l^k S_{il}(\Omega_A) S_{kj}(\Omega_B) \quad (3)$$

where Ω_A and Ω_B stand for Bader's atomic domains in the physical space,^{1,2} ${}^1D_j^i$ the spin-free first-order reduced density matrix elements and $S_{ij}(\Omega_A)$ the elements of the overlap matrix of the orthogonal molecular basis set $\{i, j, k, l, \dots\}$ over the region Ω_A ,^{32,33} the three-center bond population contributed by all possible populations shared by three centers, $I_{\Omega_A \Omega_B \Omega_C}$ as

$$\begin{aligned} \Delta_{\Omega_A \Omega_B \Omega_C}^{(3)} &= \frac{1}{4} \sum_{P(\Omega_A \Omega_B \Omega_C)} I_{\Omega_A \Omega_B \Omega_C} \\ &= \frac{1}{4} \sum_{P(\Omega_A \Omega_B \Omega_C)} \sum_{i,j,k,l,m,n} {}^1D_j^i {}^1D_l^k {}^1D_n^m S_{in}(\Omega_A) S_{kj}(\Omega_B) S_{ml}(\Omega_C) \end{aligned} \quad (4)$$

giving raise to the three-center topological bond order^{32,33} where $P(\Omega_A \Omega_B \Omega_C)$ stands for the permutations of the three domain contributions. Equation 4 represents the topological extension of the original version of 2e–3c populations.^{34,35} Also it may be noted that other interesting approaches has been recently reported.³⁶ The effectively unpaired population is quantified by^{20,29,30}

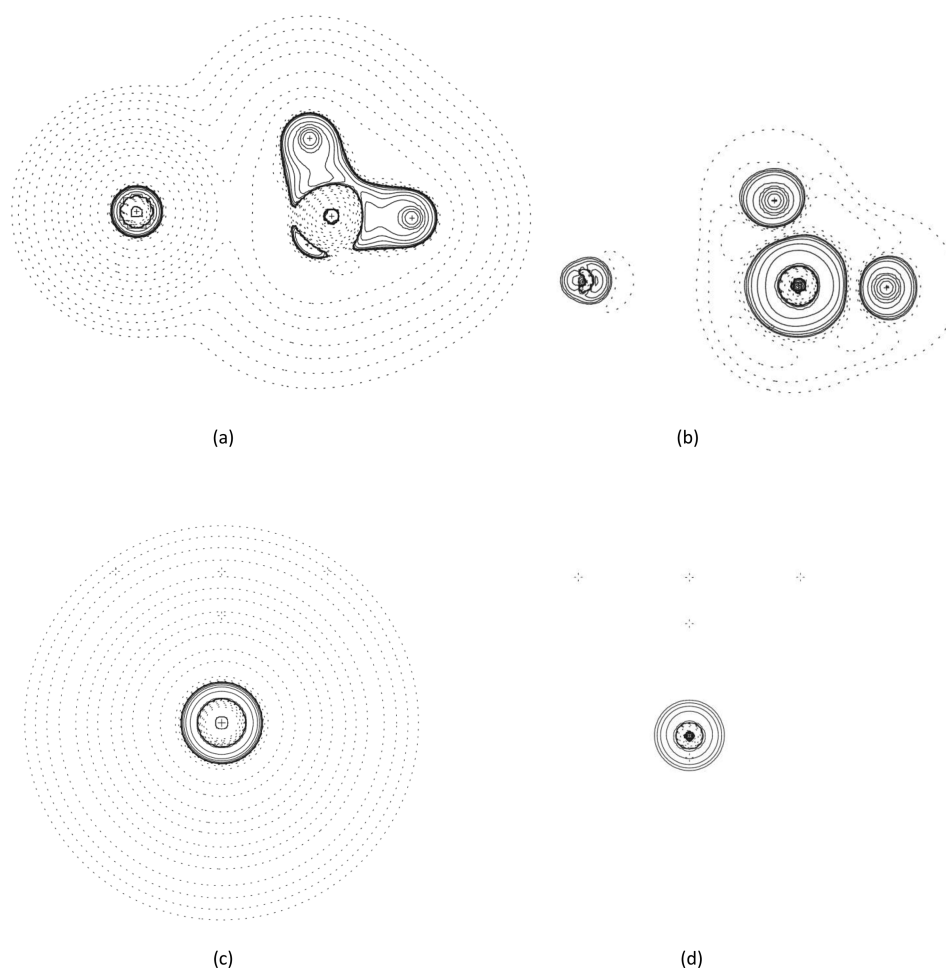


Figure 3. $L(r)$ contour maps for total density (a) and effectively unpaired densities (b) in the plane defined by C, Na ion and two of the closest H atoms and (c and d) total and effectively unpaired densities of the isolated metal ion, respectively. Positive and negative values are denoted by solid and dashed lines, respectively.

$$u_{\Omega_A} = 2 \sum_{ik} {}^1D_k^i S_{ik}(\Omega_A) - \sum_{ijkl} {}^1D_l^i {}^1D_k^j S_{ik}(\Omega_A) S_{jl}(\Omega_A) - \sum_{B \neq A} \sum_{ijkl} {}^1D_l^i {}^1D_k^j S_{ik}(\Omega_A) S_{jl}(\Omega_B) \quad (5)$$

Another fundamental concept is that of unshared populations for an atom A , Q_{Ω_A} . Its physical meaning stands for the atomic population of the inner shells and/or lone pairs in the atom, i.e., those electrons that are not involved in bonding interactions, defined by^{19,20}

$$Q_{\Omega_A} = \left[I_{\Omega_A \Omega_A} - \frac{1}{2} \sum_{\Omega_B \neq \Omega_A} I_{\Omega_A \Omega_B} \right] + \frac{1}{2} u_{\Omega_A} \quad (6)$$

where the first and second terms of the r.h.s. stand for the pairing contributions while the third one stands for the unpaired population contribution to this magnitude.

3. COMPUTATIONAL DETAILS, RESULTS, AND DISCUSSION

The state functions used in this work has been calculated at the level of configuration interaction with single and double excitations (CISD) with the basis sets 6-31G** using the Gamess04 package.³⁷ Let us note the reasons to choose the level of approximation, i.e., the statefunction and basis set. It is

worthy to note that the topological methodology for analyzing the two density fields describing the electron distribution is able to be performed for any type of statefunction with the only condition that the 1D , from which the density deserves, were N -representable.⁵ It was the case for the CISD which also provides the amount of correlation effects which converts it in an accurate method for the detailed description of the density. Other important direct methodology which incorporates correlation effects in a reliable way is the coupled cluster one (CC) but it is very difficult to obtain an N -representable 1D . Regarding the basis set it may be mentioned that although limited because of the metals in the compounds we treat in the work, the description is reliable as tested when the optimization of the several geometrical configurations for the compounds and experimental data when available is compared.^{13–15} Furthermore, because only metallic ions are used then they decrease the polarization effects. However, it states a landmark when treating higher atomic number including metals beyond the used in this work and then a basis sets including higher angular momentum quantum numbers will be needed as we have observed. The structures were optimized within this approximation and confirmed to be local minimum in the corresponding energy hypersurfaces. The densities, their critical points and their Laplacian fields $\nabla^2 \rho^{(p)}(\mathbf{r})$ and $\nabla^2 \rho^{(u)}(\mathbf{r})$ were determined by modified AIMPAC modules.³⁸ For practical reasons, $L(\mathbf{r}) = -\nabla^2 \rho(\mathbf{r})$ we will be used during the discussion

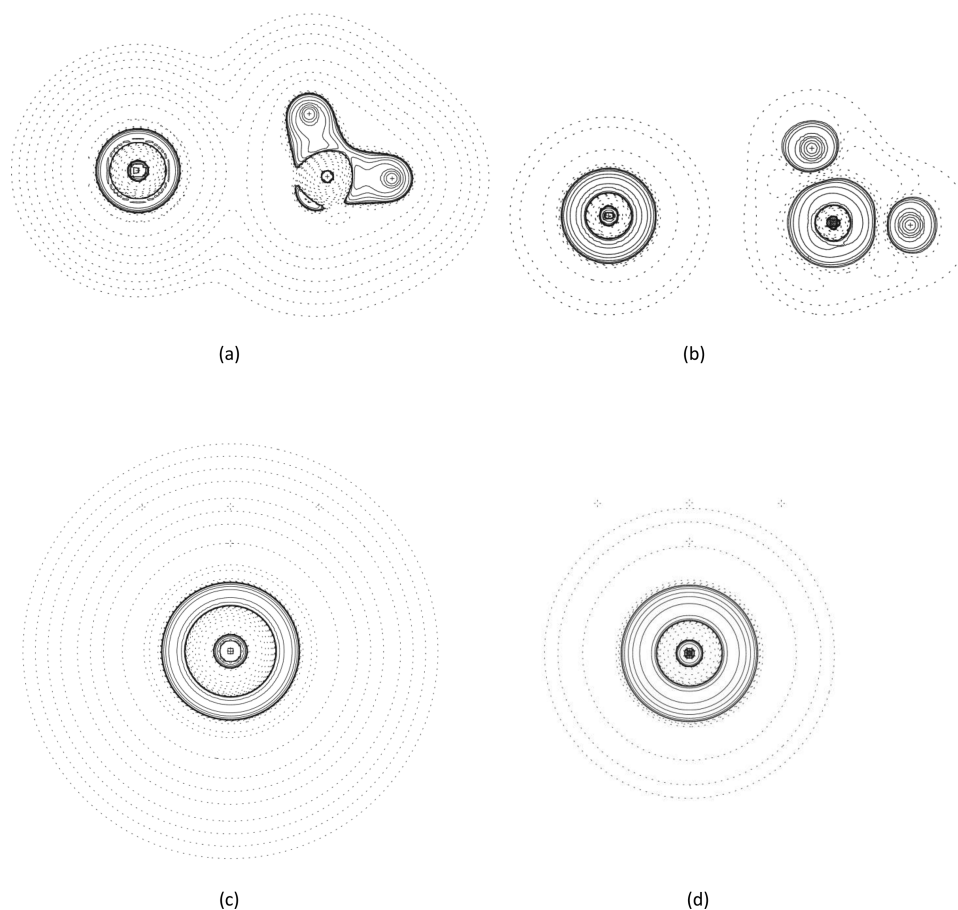


Figure 4. $L(\mathbf{r})$ contour maps for total density (a) and effectively unpaired densities (b) in the plane defined by C, K ion and two of the closest H atoms and (c and d) total and effectively unpaired densities of the isolated metal ion, respectively. Positive and negative values are denoted by solid and dashed lines, respectively.

of the results as an indicator of local concentration (positive value) or local depletion (negative value) of the number of electrons at the point of space \mathbf{r} . The terms accumulation and depletion have been proposed for the description of $\rho(\mathbf{r})$.^{1,2,39} Because of the complex structure of the $\rho^{(u)}(\mathbf{r})$ topology, we will only deal with critical points associated with its valence shells (vs) and no reference will be made to those of the inner shells of this density; in fact, only the former ones are involved in bonding phenomena. The terminology vs(3, -1)cp, vs(3, +1)cp and vs(3, +3)cp will refer to (3, -1), (3, +1) and (3, +3) valence shell critical points of $\rho^{(u)}(\mathbf{r})$ in analogy with the bcp, rcp and ccp's of the total density. It may be noted that such points are not *sensu strictu* bcp, rcp, or ccp's because only the cp's of the total density are able to define a bond in the AIM topological formalism.^{1,2} The bonding interactions has been described within the topological formalisms mentioned in the previous Section and the existence of complex interacting 2e-3c patterns in bonding are discussed in terms of the quantum rule which we have successfully built on the basis of well-known systems possessing such patterns.¹² Hence, let us introduce this rule in a general way as a 2e-3c bond interactions between atoms ABC exists if there is a vs(3, -1)cp of $\rho^{(u)}$ between each pair of atoms involved in the three-center ABC sequence and a vs(3, +1)cp defined only by the atoms involved in the three center sequence, hereafter called the local rule.¹¹ Its complementary version, hereafter the integrated or non local rule as the existence of a 2e-3c bond interactions between atoms ABC when fractional covalent bond orders $I_{\Omega_A\Omega_B}$ appear between all possible pairs of atoms AB,

BC, and AC and an appreciable $\Delta_{\Omega_A\Omega_B\Omega_C}^{(3)}$ defines its strength.¹¹

The local view may be interpreted as the indicator of the quality of the interaction between the atoms while the non local view as indicator of the strength of such interaction. It may be noted that in the cases in which $\rho^{(u)}$ vanishes identically as mentioned above, the local part collapses and consequently only three center (3c) population indicators of the interactions may be considered for the description.¹¹ As it was pointed out in the Introduction, 2e-3c type interactions has been reported for adducts formed by CH₄ alkane and alkaline/earth alkaline metallic atoms¹³ and simple clusters X₄H⁺ (X = P, As).¹⁵⁻¹⁷ Nevertheless, a more detailed study is needed to properly describe such type of interactions as shown in refs 12-14. Both sets are of different natures providing adequate examples to describe what type of interaction they undergo. This is the reason for which we choose them to apply our methodology as the first time in such type of compounds. Parts a and b of Figure 1 show the geometrical conformation of the two sets of systems of organometallic adducts and metalloid clusters, respectively.

Tables 1 and 2 contain the topological information summarizing the main parameters describing the total density $\rho(\mathbf{r})$ and the effectively unpaired density $\rho^{(u)}(\mathbf{r})$, respectively. They show the localization of their cp's and vscp's, their nature and the atomic sequence defining each of them. The non negligible values of the two-center covalent bond indices $I_{\Omega_A\Omega_B}$, three-center populations $\Delta_{\Omega_A\Omega_B\Omega_C}^{(3)}$, the unshared Q_{Ω_A} and the

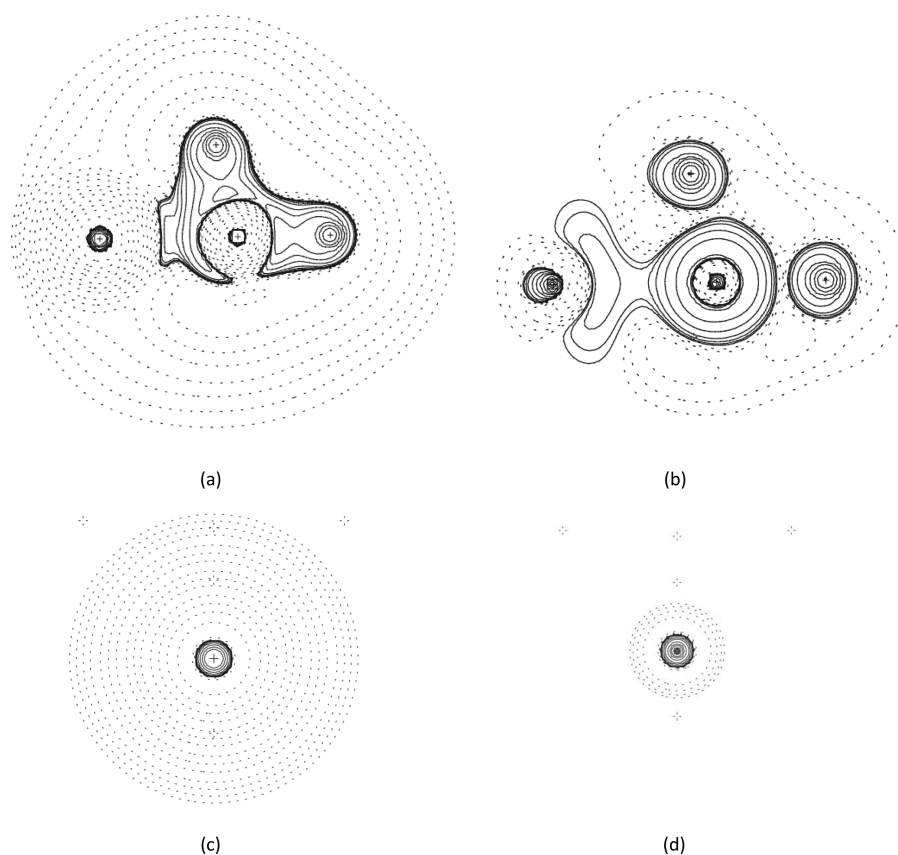


Figure 5. $L(r)$ contour maps for total density (a) and effectively unpaired densities (b) in the plane defined by C, Be ion and two of the closest H atoms and (c and d) total and effectively unpaired densities of the isolated metal ion, respectively. Positive and negative values are denoted by solid and dashed lines, respectively.

effectively unpaired populations u_{Ω_A} are shown also in these tables. No reference to the effectively paired density $\rho^{(p)}(\mathbf{r})$ is made in the tables because as shown in previous articles, its structure is similar to that of $\rho(\mathbf{r})$ and therefore it does not introduce any new information.^{11,12} Table 3 collects the values of the total and the unpaired densities and their associated Laplacian fields at the neighborhoods of the bcps and vs(3, -1) cps. The density maps shown in Figures 2–8 complete the information to describe the electron distributions.

Let us first consider the interactions for the organometallic adducts $\text{CH}_4\text{--Me}^{+p}$ ($p = 1, 2$) with Me, metallic ions of alkaline and earth alkaline metals Li, Na, K, Be, Mg, Ca in their stable gaseous phase (cf. Figure 1a). Table 1 shows that all nuclei has an associated **n**cp and all CH sequences are bonded because of the existence of a **b**cp between each pair of atoms of the CH_4 group. The most important spatial region in these systems is defined by the CMe^{+p} sequence which do present a **b**cp in all systems, i.e., there is a bonding interaction between the carbon atom and the metallic ion. Neither **r**cp nor **c**cp's arise in the distribution for these systems. All covalent bond populations I_{CH} for the alkaline atoms are very close to 0.95 (a classically single covalent bond) and slightly smaller for the CH' (outermost H atom) sequence; the same trend follow the earth alkaline atoms which exhibit slightly lower I_{CH} values in comparison with the alkaline metals and the corresponding values for the $I_{\text{CH}'}$ are markedly lower than that of the former ones. The unshared populations Q_{Ω_A} are close to the core number of electrons for each of the metal atoms. The C atom shows an unshared population close to 2.0 for the alkaline

atoms and it grows for the earth alkaline metals to values higher than 2.0, ranging from approximately 3.0 electron in Be^{+2} to 2.2 for Ca^{+2} ; i.e., this magnitude diminishes as the atom increases its atomic number. Therefore, as the metallic ions populations are very close to their core electrons, it seems that the interaction between the metallic ion and the methane produces a flow of charge from the CH bonding regions into the atomic carbon domain. The covalent bond population I_{CMe} is very low in all cases but greater for the earth alkaline atoms than that of the alkaline atoms; the 2e–3c populations for the HCMe sequence are similar for the alkaline metals, i.e., $\text{K} \approx \text{Na} \approx \text{Li}$ (cf. Table 1). For the earth alkaline metals these populations are greater than the previous with trend $\text{Ca} \approx \text{Mg} < \text{Be}$. Despite such populations are small, they are of the same order than that found for such typical interactions present in the boron hydrides.^{11,12} The results in Table 2, 3 and Figures 2–7 contain the information to analyze the validity or not of the fulfillment of the local rule based in the topology of $\rho^{(u)}$. The only candidate to undergo 2e–3c interactions is the CMeH sequence because the others lie within the stable CH_4 molecule. From Table 2 it may be noted that $\rho^{(u)}$ exhibits vs(3, -1)cps for the CMe^{+p} and for the CH sequences but such vscps are not present for HMe^{+p} within the CMe^{+p}H sequences and there are no vs(3, +1)cps. Therefore, the local rules are not fulfilled, and no 2e–3c interactions are detected for these adduct conformations. Despite the systems are electron deficient compounds, the metallic ions do not generate an enough attraction of the electron cloud from the methane to expand unpaired electron density through space (TS) in order to be the onset of the 2e–3c interaction as may be observed

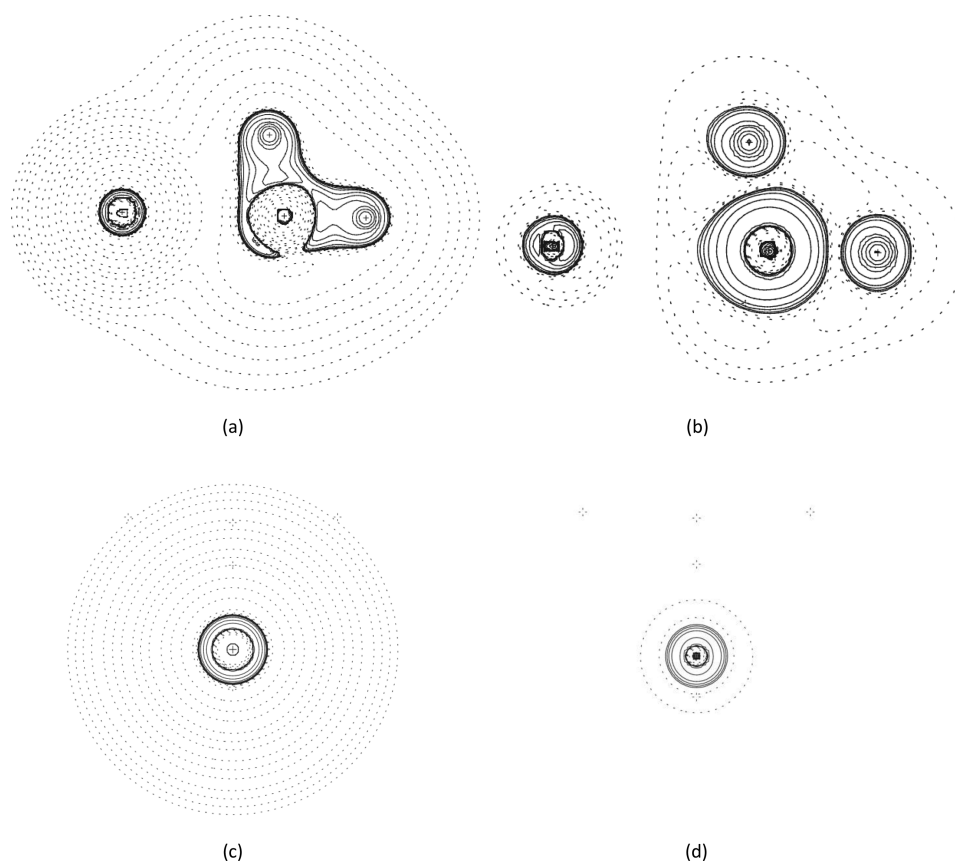


Figure 6. $L(r)$ contour maps for total density (a) and effectively unpaired densities (b) in the plane defined by C, Mg ion and two of the closest H atoms and (c and d) total and effectively unpaired densities of the isolated metal ion, respectively. Positive and negative values are denoted by solid and dashed lines, respectively.

from Figures 2b–7b.¹² Comparison of metal ion within the adduct and the isolated ion atomic densities in Figures 2c,d–7c,d show that the paired densities do not exhibit any change while a notably polarization redistribution is observed for the unpaired part being much important for the lower atomic number.

Table 3 permits one to observe the accumulation of ρ and depletion of $\rho^{(u)}$ at their bcp for the CH sequences of methane closer to the metal ion showing the typical feature for a covalent bond interaction,^{7,8} i.e., positive L at the bcp.¹ Nevertheless, the outermost hydrogen atom H' shows also accumulation of $\rho^{(u)}$ for the earth alkaline metallic ions of lower atomic number very marked for Be, very small for Mg becoming typical covalent for Ca.⁸ These features are in agreement with the lower covalent population for the sequence CH' in comparison with that of CH. The atomic unpaired populations u_{Ω_A} show an appreciable value for K and Ca, those of greater atomic number for both alkaline and earth alkaline metals, respectively, in comparison with all other ions which do not differ too much between them. It is in close agreement with the very expanded unpaired core electron density shown in Figures 4b and 7b. The sequences CMe^{+p} interactions show depletion for ρ and $\rho^{(u)}$ at bcps for all metals and therefore may be considered as closed shell interactions, i.e., negative L at the bcp.¹ An exception is the Be ions where local increment for $\rho^{(u)}$ is found which agrees with the corresponding map for the unpaired density showing an appreciable "spillage" over the interatomic CBe domain (cf. Figure 5b). However, this interaction is not enough to build a $\text{vs}(3, +1)_{cp}$ (cf. Table 2)

and so it can not be classified as through space (TS).¹² Hence, the ion metals are nothing but a core and thus the only possible interaction is the electrostatic producing a charge flux as described above and consequently no complex patterns such as 2e–3c ones appear for these distributions, i.e., the group CH_4 is not able to share electrons with the metal ion so that they can not undergo 3c interactions. However, because of the flux of charge expressed as a decrement of bond orders of the CH and CH' sequences, as explained above, are responsible for the CMe^{+p} interaction, i.e., CMe^{+p} interactions are CH assisted. The behavior of the pairing densities are shown in Figures 2a–7a. These maps show similar pairing accumulations between for CH sequences in all systems and marked depletion for the C–Me⁺ sequences in agreement with the results of the integrated magnitudes values and the classification as shared and closed shell interactions respectively, through the local analysis. Hence, the local rule is not fulfilled for any of the sequences in these type of adducts.

The second group resembles an example of simple clusters X_4H^+ ($\text{X} = \text{P}, \text{As}$) with experimental support about the existence of 2e–3c interactions.^{15,16} Table 1 show the topological analysis of the electronic structure of X_4H^+ ($\text{X} = \text{P}, \text{As}$) clusters schematically shown in Figure 1b. The physical conformation is essentially composed by a bridge domain formed by two of the X_{hb} atoms and a H one (superior part of the Figure) plus two other X atoms not involved in the bridge (inferior part of the Figure) forming the cluster. There is no bonding interaction between the head-bridge X_{hb} atoms (P or As), i.e., there are no bcp's between P_{hb} or As_{hb} atoms in the

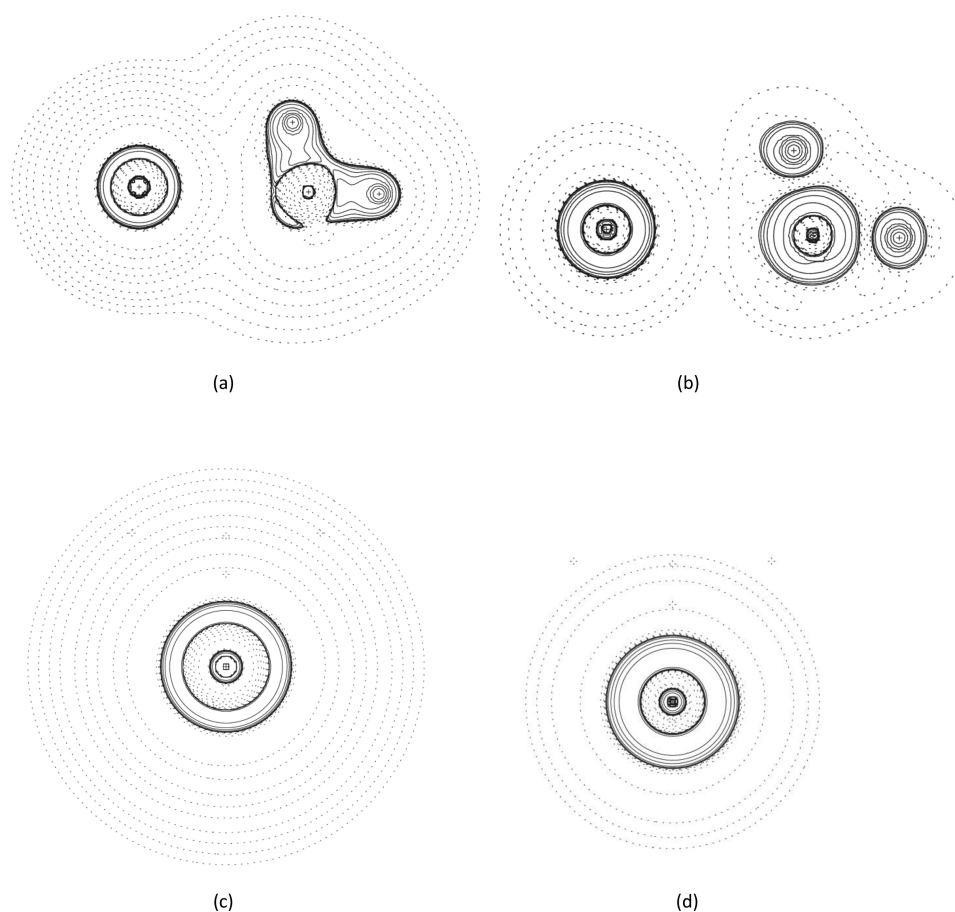


Figure 7. $L(r)$ contour maps for total density (a) and effectively unpaired densities (b) in the plane defined by C, Ca ion and two of the closest H atoms and (c and d) total and effectively unpaired densities of the isolated metal ion, respectively. Positive and negative values are denoted by solid and dashed lines, respectively.

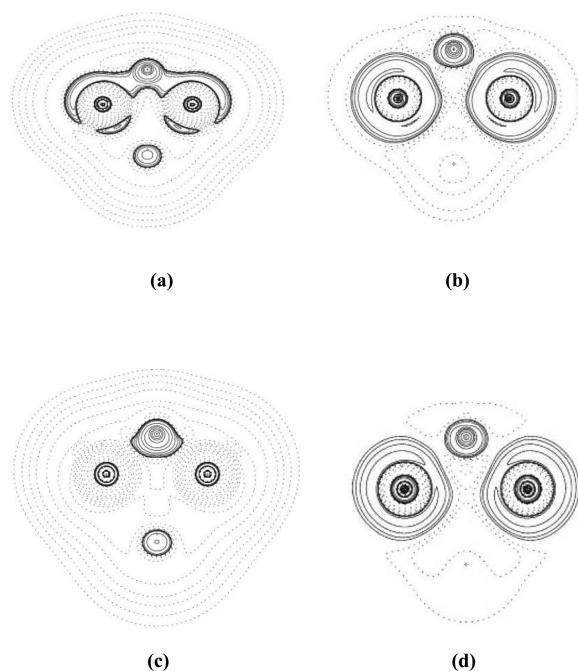


Figure 8. $L(r)$ contour maps for total density (a) and effectively unpaired densities (b) in the plane defined by H, and the head-bridge P atoms; (c and d) idem for As clusters.

bridge. Bonding interactions are present between the X_{hb} atoms and H in the bridge domain. Moreover, the system exhibits the presence of *rcp* formed by each of the $X_{hb}XX_{hb}H$ and $XX_{hb}X$ sequences. The $X_{hb}XXX_{hb}$ sequence defines a *ccp*'s indicating a subtle interaction emerging from the cluster structure. It is worthy to note that the H atom only belongs to both possible rings mentioned above, i.e., $X_{hb}XX_{hb}H$ for each of the non-bridge X atoms but no to the cage structure at the topological total density level of description. The covalent bond orders $I_{X_{hb}X}$ and I_{XX} are very close to an integer number, in these cases 1.0 which indicates a single bond in classical terms. Nevertheless, the bridge $I_{X_{hb}H}$ and $I_{X_{hb}X_{hb}}$ are fractional. The $2e-3c$ populations $\Delta_{\Omega_A\Omega_B\Omega_C}$ for the three possible sequences between atoms in this clusters shown in Table 1 are non-negligible and very similar each other. All this information permits to conclude that the nonlocal rule is fulfilled for the electron distribution of this group only for the bridge; i.e., only $2e-3c$ interactions are present for the sequence $X_{hb}HX_{hb}$. The local analysis constitutes the most subtle information about the electronic structure of the clusters and is summarized in Table 2. We may appreciate there that only atomic interactions of $2e-3c$ type are present for the sequence $X_{hb}HX_{hb}$ because of the existence of $vs(3, -1)cp$ between each of the atom in the sequence and a $vs(3, +1)cp$ between the three atoms involved. The same is not true for any of the other sequences involving only X atoms different of X_{hb} and H atoms. Therefore, the rule only follows for that sequence. Parts a and b of Figure 8 show the total and unpaired

Table 1. Electronic Structure of Organometallic Adducts $\text{CH}_4\text{--Me}^+$ (Me = Li, Na, K, Be, Mg, Ca) and X_4H^+ (X = P, As) Clusters^a

cp type	ρ sequences ^b	bond	$I_{\Omega_a\Omega_b}$	3c-sequence	$\Delta_{\Omega_a\Omega_b\Omega_c}^{(3)}$
CH_4Li^+					
ncp	one on each atom				
bcp	one on each CH sequence ^c	CH	0.950 (0.915)		
	one on the CLi sequence	CLi	0.037		
		LiH	0.008 (0.007)		
rcp	not present			HLiC	0.011
ccp	not present				
CH_4Na^+					
ncp	one on each atom				
bcp	one on each CH sequence ^c	CH	0.951 (0.925)		
	one on the CNa sequence	CNa	0.038		
		NaH	0.010 (0.007)		
rcp	not present			HNaC	0.011
ccp	not present				
CH_4K^+					
ncp	one on each atom				
bcp	one on each CH sequence ^c	CH	0.954 (0.937)		
	one on the CK sequence	CK	0.033		
		KH	0.010 (0.006)		
rcp	not present			HKC	0.010
ccp	not present				
$\text{CH}_4\text{Be}^{+2}$					
ncp	one on each atom				
bcp	one on each CH sequence ^c	CH	0.900 (0.793)		
	one on the CBe sequence	CBe	0.177		
		BeH	0.026 (0.020)		
rcp	not present			HBeC	0.045
ccp	not present				
$\text{CH}_4\text{Mg}^{+2}$					
ncp	one on each atom				
bcp	one on each CH sequence ^c	CH	0.940 (0.840)		
	one on the CMg sequence	CMg	0.127		
		MgH	0.022 (0.021)		
rcp	not present			HMgC	0.034
ccp	not present				
$\text{CH}_4\text{Ca}^{+2}$					
ncp	one on each atom				
bcp	one on each CH sequence ^c	CH	0.943 (0.880)		
	one on the CCa sequence	CCa	0.115		
		CaH	0.028 (0.017)		
rcp	not present			HCaC	0.035
ccp	not present				
P_4H^+					
ncp	one on each atom				
bcp	not present for $\text{P}_{hb}\text{P}_{hb}$ ^d	$\text{P}_{hb}\text{P}_{hb}$	0.526		
	one on each P_{hb}P sequence	P_{hb}P	1.026		
	one on the PP sequence	PP	0.994		
	one on each P_{hb}H sequence	P_{hb}H	0.547		
rcp	one for each $\text{P}_{hb}\text{HP}_{hb}\text{P}$ sequence			$\text{P}_{hb}\text{HP}_{hb}$	0.185
ccp	one for each PP_{hb}P sequence			PP_{hb}P	0.171
	one for the $\text{P}_{hb}\text{PPP}_{hb}$ sequence			$\text{P}_{hb}\text{PPP}_{hb}$	0.153
As_4H^+					
ncp	one on each atom				
bcp	not present for $\text{As}_{hb}\text{As}_{hb}$ ^d	$\text{As}_{hb}\text{As}_{hb}$	0.493		
	one on each As_{hb}As sequence	As_{hb}As	1.035		
	one on the AsAs sequence	AsAs	1.012		
	one on each As_{hb}H sequence	As_{hb}H	0.552		
rcp	one for each $\text{As}_{hb}\text{HAS}_{hb}\text{As}$ sequence			$\text{As}_{hb}\text{HAS}_{hb}$	0.190
	one for each $\text{AsAs}_{hb}\text{As}$ sequence			$\text{AsAs}_{hb}\text{As}$	0.164

Table 1. continued

cp type	ρ sequences ^b	bond	I_{Ω,Ω_B}	3c-sequence	$\Delta_{\Omega,\Omega_B,\Omega_C}^{(3)}$
		As ₄ H ⁺			
ccp	one for the As _{hb} AsAsAs _{hb} sequence			As _{hb} AsAs _{hb}	0.150

^aLocal and integrated (non-local) topological features of $\rho(r)$ density at CISD/6-31G** level of approximation. All quantities are in atomic units.

^bIndicate the nucleus at which the **n**cp is located; for **bcps**, the atoms defining the bond; for **rcps**, the atoms giving rise to the ring; for **ccps**, the atoms defining the cage. The sequence involving H atoms corresponds to those closer to the metal ion. ^cCH sequence in CH₃ group (values between parentheses correspond to the CH sequence of the outmost H atom) (see Figure 1). ^dAs_{hb} and P_{hb} stands for the head-bridge atoms in the P_{hb}HP_{hb} or As_{hb}HAs_{hb} sequences (see text and Figure 1).

Laplacian maps in the plane containing the sequence X_{hb}HX_{hb}, respectively and then because of their “spillage”, 2e–3c interactions in both systems pertains to the TS type distribution.¹² The values for the unshared populations Q_{Ω_A} , approximately 11.5 for P atoms and 29.5 for As atoms are in agreement with the number of core electrons of 10 and 28 for P and As atoms, respectively. The unpaired density maps (cf. Figure 8) and their associated populations u_{Ω_A} in Table 2 are according to the TS type distribution.^{11,12} Let us analyze the information about the densities and $L(r)$ at bcp and vs(3, –1)cp in Table 3. X_{hb}H sequences show accumulation for ρ and $\rho^{(u)}$ at the bcp in P case and a very small depletion for As case which may be globally observed from the maps in Figure 8 indicating a non typical covalent interaction in agreement with the 2e–3c interactions described above. Other interesting information is that the similar values of ρ and $\rho^{(u)}$ evaluated at both critical points indicate their proximity.⁷ The XX as well as X_{hb}X sequences exhibit typical covalent interactions as described by the accumulation of the pairing density and the depletion of the unpaired one⁷ and the values of the corresponding covalent bond orders (cf. Table 1).

4. CONCLUDING REMARKS

In this work, we deal with two types of simple compounds that differ essentially in their electronic nature which were not described up to now by means of a detailed topological methodology. The first group of these compounds lies within the most simple organometallic ion adduct interactions while the second set exemplifies a cluster type interaction of metalloids. As a whole they provided enough information to depict the essential knowledge about the nature of the nonclassical interactions and consequently permits to gain some new insight about the application of local topological methods beyond the traditional electron density distributions.

The present organometallic adducts are electron-deficient compounds and thus candidates to exhibits 2e–3c interactions. As indicated by the detailed results describing their distribution, it is shown that they are not able to transfer charge from the embedded metallic ion core toward the CH₄ group and only a unpaired density cloud polarization as may be observed from the accumulation/depletion maps (Figures 2–7). Because of the analysis which indicates that both parts of the rule are not fulfilled it may be concluded that the electronic distribution of these systems has only 2e–2c patterns, and no 2e–3c complex patterns of bonding appear.

The second group of compounds considered, those of interacting metalloid-hydrogen clusters has been previously studied and exhibit experimental evidence for the onset of 2e–3c interactions as noted in the Introduction section. The detailed analysis exposed in the previous section allows to conclude that 2e–3c interactions are present in these systems only in the bridge domain, i.e., between the two head-bridge

metalloid atoms (P or As) and the hydrogen atom and belong to the TS type. No such interactions are present between three metalloid atoms in agreement with the mentioned experimental results.

The behavior of metal and metalloid like systems reinforce the global conclusion which can be condensed in that the knowledge about 2e–3c many-atoms interactions is supported by the $\rho^{(u)}$ density localization concept and the onset of its vscp's. Consequently, all these results provides a natural scenario for the application of these techniques to more complex electron distributions in organometallic chemistry as for instance, the back-donation phenomena, which among others are being considered in our laboratories.

AUTHOR INFORMATION

Corresponding Authors

*E-mail: rmlb@exa.unne.edu.ar (R.M.L.).

*E-mail: rboc@df.uba.ar (R.C.B.).

Notes

The authors declare no competing financial interest.

ACKNOWLEDGMENTS

This report has been financially supported by Projects 20020130100226BA (Universidad de Buenos Aires) and PIP No. 11220090100061 (Consejo Nacional de Investigaciones Científicas y Técnicas, República Argentina). R. M. L. acknowledges financial support of the Secretaria General de Ciencia y Técnica de la Universidad Nacional del Nordeste (Corrientes, Argentina) and facilities provided during the course of this work.

REFERENCES

- (1) Bader, R. F. W. *Atoms in Molecules: A Quantum Theory*; Clarendon Press: Oxford, U.K., 1994.
- (2) Popelier, P. L. A. *Atoms in Molecules: An Introduction*; Pearson Educ.: London, 1999.
- (3) Bamzai, A. S.; Deb, B. M. The role of single-particle density in chemistry. *Rev. Mod. Phys.* **1981**, *53*, 95–126; Erratum. *Rev. Mod. Phys.* **1981**, *53*, 593.
- (4) Parr, R. G.; Yang, W. *Density-Functional Theory of Atoms and Molecules*; Oxford University Press: New York, 1989.
- (5) Coleman, A. J.; Yukalov, V. I. *Reduced Density Matrices: Coulson's Challenge*; Springer-Verlag: New York, 2000.
- (6) Bader, R. F. W. Bond Paths Are Not Chemical Bonds. *J. Phys. Chem. A* **2009**, *113*, 10391–10396.
- (7) Lobayan, R. M.; Bochicchio, R. C.; Lain, L.; Torre, A. Electron-density topology in molecular systems: Paired and unpaired densities. *J. Chem. Phys.* **2005**, *123*, 144116.
- (8) Lobayan, R. M.; Bochicchio, R. C.; Lain, L.; Torre, A. Laplacian Field of the Effectively Unpaired Electron Density: Determination of Many-Body Effects on Electron Distributions. *J. Phys. Chem. A* **2007**, *111*, 3166–3172.
- (9) Wade, K. *Electron Deficient Compounds. Studies in Modern Chemistry*; T. Nelson and Sons Ltd.: London, 1971.

Table 2. Electronic Structure of Organometallic Adducts $\text{CH}_4\text{--Me}^+$ (Me = Li, Na, K, Be, Mg, Ca) and X_4H^+ (X = P, As) Clusters^a

cp type	$\rho^{(u)}$ sequences ^b	atom	Q_{Ω_i}	u_{Ω_i} ^c
CH_4Li^+				
vs (3, -3) cp	one on each atom	C	2.173	0.199
		H	-0.055 (-0.130)	0.065 (0.062)
		Li	1.964	0.017
vs (3, -1) cp	one for each CH sequence			
	one for LiC sequence			
vs (3, +1) cp	not present			
vs (3, +3) cp	not present			
CH_4Na^+				
vs (3, -3) cp	one on each atom	C	2.109	0.194
		H	-0.044 (-0.121)	0.070 (0.051)
		Na	9.961	0.024
vs (3, -1) cp	present on each CH sequence			
	present for NaC sequence			
vs (3, +1) cp	not present			
vs (3, +3) cp	not present			
CH_4K^+				
vs (3, -3) cp	one on each atom	C	2.057	0.199
		H	-0.035 (-0.116)	0.060 (0.051)
		K	17.924	0.244
vs (3, -1) cp	present on each CH sequence			
	present for KC sequence			
vs (3, +1) cp	not present			
vs (3, +3) cp	not present			
$\text{CH}_4\text{Be}^{2+}$				
vs (3, -3) cp	one on each atom	C	3.037	0.247
		H	-0.167 (-0.228)	0.055 (0.038)
		Be	1.875	0.046
vs (3, -1) cp	present on each CH sequence			
	present for BeC sequence			
vs (3, +1) cp	not present			
vs (3, +3) cp	not present			
$\text{CH}_4\text{Mg}^{2+}$				
vs (3, -3) cp	one on each atom	C	2.486	0.205
		H	-0.111 (-0.206)	0.060 (0.046)
		Mg	9.898	0.045
vs (3, -1) cp	present on each CH sequence			
	present for MgC sequence			
vs (3, +1) cp	not present			
vs (3, +3) cp	not present			
$\text{CH}_4\text{Ca}^{2+}$				
vs (3, -3) cp	one on each atom	C	2.220	0.186
		H	-0.070 (-0.177)	0.060 (0.048)
		Ca	17.866	0.274
vs (3, -1) cp	present on each CH sequence			
	present for CaC sequence			
vs (3, +1) cp	not present			
vs (3, +3) cp	not present			
P_4H^+				
vs (3, -3) cp	one on each atom	P_{hb}^d	11.520	0.290
		P^e	11.610	0.300
		H	0.017	0.085
vs (3, -1) cp	one for each P_{hb}P sequence			
	one for each $\text{P}_{hb}\text{P}_{hb}$ sequence			
	one for each PP sequence			
	one for each P_{hb}H sequences			
vs (3, +1) cp	one for $\text{P}_{hb}\text{PP}_{hb}$ sequences			
	one for PP_{hb}P sequences			
vs (3, +3) cp	not present			

Table 2. continued

cp type	$\rho^{(u)}$ sequences ^b	atom	Q_{Ω_i}	u_{Ω_i} ^c
		As ₄ H ⁺		
vs (3, -3) cp	one on each atom	As _{hb} ^d	29.507	0.259
		As ^e	29.578	0.261
		H	0.036	0.057
vs (3, -1) cp	one for each As _{hb} As sequence one for each As _{hb} As _{hb} sequence one for each AsAs sequence one for each As _{hb} H sequences			
vs (3, +1) cp	one for As _{hb} AsAs _{hb} sequences one for AsAs _{hb} As sequences			
vs (3, +3) cp	not present			

^aLocal and integrated (non-local) topological features of $\rho^{(u)}(\mathbf{r})$ density at CISD/6-31G** level of approximation. All quantities are in atomic units.

^bIndicate the nucleus at which the vs(3, -3)cp is located; for vs(3, -1)cps, the atoms defining the bond; for vs(3, +1)cps, the atoms giving rise to the ring; for vs(3, +1)cps, the atoms defining the cage. ^cEffectively unpaired atomic electron population. ^dBridgehead atom (see Table 1). ^eAtoms not involved in the bridge.

(10) Lobayan, R. M.; Bochicchio, R. C.; Torre, A.; Lain, L. Topology of the Effectively Paired and Unpaired Electron Densities for Complex Bonding Patterns: The Three-Center Two-Electron Bonding Case. *J. Chem. Theor. Comp.* **2009**, *5*, 2030–2043. and references therein.

(11) Lobayan, R. M.; Bochicchio, R. C.; Torre, A.; Lain, L. Electronic Structure and Effectively Unpaired Electron Density Topology in closo-Boranes: Nonclassical Three-Center Two-Electron Bonding. *Chem. Theor. Comp.* **2011**, *7*, 979–987. and references therein.

(12) Lobayan, R. M.; Bochicchio, R. C. Pairing and unpairing electron densities in organic systems: Two-electron three center through space and through bonds interactions. *J. Chem. Phys.* **2014**, *140*, 174302. and references therein.

(13) Sundberg, M. R.; Zborowski, K. K.; Alkorta, I. Multiple 3c-2e bonding of methane with metal cations. *Chem. Phys. Lett.* **2011**, *515*, 210–213.

(14) Hall, C.; Perutz, R. N. Transition Metal Alkane Complexes. *Chem. Rev.* **1996**, *96*, 3125–3146. and references.

(15) Abboud, J. L. M.; Herreros, M.; Notario, R.; Esseffar, M.; M^o, O.; Yañez, M. A New Bond from an Old Molecule: Formation, Stability, and Structure of P₄H⁺. *J. Am. Chem. Soc.* **1996**, *118*, 1126–1130.

(16) Alcamí, M.; M^o, O.; Yañez, M. Ab initio and density functional theory calculations on the protonated species of As₄ clusters. *J. Chem. Phys.* **1998**, *108*, 8957–8963.

(17) Bochicchio, R. C.; Lain, L.; Torre, A.; Ponec, R. Picture of Bonding in Protonated Phosphorus and Arsenic Clusters. Detection of 3-Center Bonds from the Generalized Population Analysis. *Croat. Chem. Acta* **2000**, *73*, 1030–1046.

(18) Bochicchio, R. C. Quantum Statistical Nature of the Chemical Bond. Part I. Theoretical framework of population analysis and application to SCF closed shell wavefunctions. *J. Mol. Struct.: THEOCHEM* **1991**, *228*, 209–225. and references therein.

(19) Bochicchio, R. C.; Lain, L.; Torre, A. On the definition of bond orders at correlated level. *Chem. Phys. Lett.* **2003**, *374*, 567–571. and references therein.

(20) Bochicchio, R. C.; Lain, L.; Torre, A. Atomic valence in molecular systems. *Chem. Phys. Lett.* **2003**, *375*, 45–53. and references therein.

(21) Torre, A.; Lain, L.; Bochicchio, R. C. Bond Orders and Their Relationships with Cumulant and Unpaired Electron Densities. *J. Phys. Chem. A* **2003**, *107*, 127–130.

(22) Lain, L.; Torre, A.; Bochicchio, R. C. Studies of Population Analysis at the Correlated Level: Determination of Three-Center Bond Indices. *J. Phys. Chem. A* **2004**, *108*, 4132–4137.

(23) McWeeny, R. *Methods of Molecular Quantum Mechanics*; Academic: London, 1969.

(24) Davidson, E. D. *Reduced Density Matrices in Quantum Chemistry*; Academic: New York, 1976.

(25) Bachrach, S. M. Population Analysis and Electron Densities from Quantum Mechanics. *Rev. Comput. Chem.* **1994**, *5*, 171–227.

(26) Lobayan, R. M.; Alcoba, D. R.; Bochicchio, R. C.; Torre, A.; Lain, L. Topology of the Electron Density in Open-Shell Systems. *J. Phys. Chem. A* **2010**, *114*, 1200–1206.

(27) Takatsuka, K.; Fueno, T.; Yamaguchi, K. Distribution of odd electrons in ground-state molecules. *Theor. Chim. Acta* **1978**, *48*, 175–183.

(28) Takatsuka, K.; Fueno, T. The spin-optimized SCF general spin orbitals. II. The 2 ²S and 2 ²P states of the lithium atom. *J. Chem. Phys.* **1978**, *69*, 661–669.

(29) Bochicchio, R. C. On spin density and hole distribution relations: valence and free valence. *J. Mol. Struct.: THEOCHEM* **1998**, *429*, 229–236.

(30) Staroverov, V. N.; Davidson, E. R. Distribution of effectively unpaired electrons. *Chem. Phys. Lett.* **2000**, *330*, 161–168.

(31) Fradera, X.; Austen, M. A.; Bader, R. F. W. The Lewis Model and Beyond. *J. Phys. Chem. A* **1999**, *103*, 304–314.

(32) Bochicchio, R. C.; Lain, L.; Torre, A.; Ponec, R. Topological population analysis from higher order densities. I. Hartree-Fock level. *J. Math. Chem.* **2000**, *28*, 83–90.

(33) Torre, A.; Lain, L.; Bochicchio, R. C.; Ponec, R. Topological population analysis from higher order densities II. The correlated case. *J. Math. Chem.* **2002**, *32*, 241–248.

(34) Giambiagi, M.; de Giambiagi, M. S.; Mundim, K. C. Definition of a Multicenter Bond Index. *Struct. Chem.* **1990**, *1*, 423–427.

(35) Ponec, R.; Mayer, I. Investigation of some Properties of Multicenter Bond Indices. *Phys. Chem. A* **1997**, *101*, 1738–1741.

(36) Feixas, F.; Solà, M.; Barroso, J. M.; Ugalde, J. M.; Matito, E. New approximation to the third-order density. Application to the calculation of correlated multicenter indices. *J. Chem. Theor. Comput.* **2014**, *10*, 3055–3065.

(37) Schmidt, M. W.; Baldridge, K. K.; Boatz, J. A.; Elbert, S. T.; Gordon, M. S.; Jensen, J. H.; Koseki, S.; Matsunaga, N.; Nguyen, K. A.; Su, J. S.; Windus, T. L.; Dupuis, M.; Montgomery, J. A. General atomic and molecular electronic structure system. *J. Comput. Chem.* **1993**, *14*, 1347–1363.

(38) Biegler-König, F. W.; Bader, R. F. W.; Tang, T. H. Calculation of the average properties of atoms in molecules. II. *J. Comput. Chem.* **1982**, *3*, 317–328.

(39) Popelier, P. L. A. On the full topology of the Laplacian of the electron density. *Coord. Chem. Rev.* **2000**, *197*, 169–189.

Table 3. Density and $L(r)$ of the Total Density ρ and $\rho^{(u)}$ for Organometallic Adducts $\text{CH}_4\text{--Me}^+$ ($\text{Me} = \text{Li}, \text{Na}, \text{K}, \text{Be}, \text{Mg}, \text{Ca}$) and X_4H^+ ($\text{X} = \text{P}, \text{As}$) Clusters at Bond Critical Points of the Total Density at CISD/6-31G** Level of Calculation^a

system ^b	bond	$\rho(\mathbf{r}) _{\text{bcp}}$	$\rho^{(u)}(\mathbf{r}) _{\text{bcp}}$	$-\nabla^2 \rho(\mathbf{r}) _{\text{bcp}}$	$-\nabla^2 \rho^{(u)}(\mathbf{r}) _{\text{bcp}}$	ε^c	
CH ₄ –Li ⁺	CLi	0.01524	0.00039	−0.10074	−0.00026	0.00004	
		0.11412	0.00387	−0.15422	0.00022	0.00013	
	CH ^{'d}	0.28301	0.00582	1.05166	−0.00508	0.00001	
		0.28344	0.00586	1.01233	−0.00568	0.00006	
	CH	0.27438	0.00582	0.94214	−0.00500	0.03256	
		0.27391	0.00574	0.95821	−0.00515	0.03021	
CH ₄ –Na ⁺	CNa	0.01076	0.00027	−0.06034	−0.00024	0.00034	
		0.05583	0.00172	−0.12648	−0.00263	0.00013	
	CH ^{'d}	0.28352	0.00577	1.04367	−0.00561	0.00001	
		0.28378	0.00581	1.01486	−0.00588	0.00000	
	CH	0.27629	0.00581	0.95149	−0.00501	0.02310	
		0.27521	0.00571	0.97344	−0.00519	0.03001	
CH ₄ –K ⁺	CK	0.00718	0.00020	−0.03293	−0.00054	0.00016	
		0.02143	0.00054	−0.06538	−0.00148	0.00009	
	CH ^{'d}	0.28574	0.00511	1.05348	−0.00533	0.00000	
		0.28585	0.00513	1.03516	−0.00541	0.00000	
	CH	0.27935	0.00517	0.97730	−0.00453	0.01573	
		0.27785	0.00505	1.00515	−0.00454	0.02774	
CH ₄ –Be ²⁺	CBe	0.08274	0.00248	−0.44012	0.00533	0.00001	
		0.09536	0.00304	−0.02758	0.00384	0.00000	
	CH ^{'d}	0.26371	0.00632	1.09431	0.73682	0.00000	
		0.26816	0.00612	0.00167	0.90992	0.00000	
	CH	0.25274	0.00574	0.81345	−0.29548	0.13196	
		0.25220	0.00580	0.77783	−0.00302	0.02682	
CH ₄ –Mg ²⁺	CMg	0.03299	0.00081	−0.19089	−0.00009	0.00142	
		0.03197	0.00450	−0.05233	0.00285	0.00008	
	CH ^{'d}	0.26953	0.00609	1.03707	0.00109	0.00003	
		0.27164	0.00604	0.92729	−0.00312	0.00006	
	CH	0.26565	0.00580	0.88746	−0.00404	0.07329	
		0.26580	0.00581	0.88401	−0.00403	0.02350	
CH ₄ –Ca ²⁺	CCa	0.02323	0.00056	−0.10348	−0.00204	0.00024	
		0.06551	0.00173	−0.10300	−0.00187	0.00001	
	CH ^{'d}	0.28183	0.00514	1.09328	−0.00263	0.00005	
		0.28309	0.00515	1.01434	−0.00471	0.00002	
	CH	0.27303	0.00511	0.93160	−0.00409	0.04990	
		0.27298	0.00506	0.95281	−0.00411	0.03308	
P ₄ H ⁺	PH(bridge)	0.11039	0.00293	0.15150	0.00216	0.17298	
		0.11172	0.00282	0.13714	0.00011	0.00277	
	P _{hb} P _{hb} ^{ef}	no bcp					
		0.06748	0.00157	−0.08923	−0.00340	0.06033	
	pp ^g		0.12069	0.00262	0.14664	−0.00185	0.09510
			0.12034	0.00261	0.13671	−0.00202	0.09204
As ₄ H ⁺	P _{hb} P ^h		0.10903	0.00244	0.09532	−0.00242	0.00655
			0.10874	0.00245	0.08767	−0.00237	0.03175
	AsH(bridge)		0.09307	0.00224	−0.00889	−0.00005	0.11939
			0.09240	0.00225	−0.01701	0.00054	0.08596
	As _{hb} As _{hb} ^{ef}	no bcp					
			0.05119	0.00134	−0.06811	−0.00177	0.16190
	AsAs ^g		0.08763	0.00185	0.04981	−0.00114	0.10172
			0.08741	0.00185	0.04739	−0.00117	0.08537
	As _{hb} As ^h		0.08012	0.00178	0.03524	−0.00120	0.01181
			0.07997	0.00179	0.03071	−0.00120	0.04027

^aSecond line in columns 3–7 for each bond indicates the densities and $L(r)$ at $\rho^{(u)}(r)$ vs(3, −1)cp. All quantities are in atomic units ^bSee Figure 1 for atoms labeling. ^cEllipticity. ^dH', H indicate the hydrogen atoms which are outermost and closer to the ligand metal, respectively. ^eThere are no bcp points for $\rho(r)$ between these atoms. ^f P_{hb} or As_{hb} atoms closer to the H atom (bridge). ^gP or As more distant atoms to the H atom. ^hP or As atoms closer and outermost to the H atom.